Biochimica et Biophysica Acta 1838 (2014) 2306–2312

Contents lists available at ScienceDirect

Biochimica et Biophysica Acta

journal homepage: www.elsevier.com/locate/bbamem

Utilizing zeta potential measurements to study the effective charge, membrane partitioning, and membrane permeation of the lipopeptide surfactin ☆

Helen Y. Fan [a], Mozhgan Nazari [a], Gaurav Raval [a], Zubeir Khan [a], Hiren Patel [a], Heiko Heerklotz [a,b,*]

[a] Leslie Dan Faculty of Pharmacy, University of Toronto, 144 College st, Toronto, ON M5S3M2, Canada
[b] Institute for Medical Physics and Biophysics, University of Leipzig, Leipzig, Germany

ARTICLE INFO

Article history:
Received 10 January 2014
Accepted 21 February 2014
Available online 11 March 2014

Keywords:
Zeta potential
Lipopeptide
Antimicrobial
Membrane partitioning
Membrane permeation

ABSTRACT

The effective charge of membrane-active molecules such as the fungicidal lipopeptide surfactin (SF) is a crucial property governing solubility, membrane partitioning, and membrane permeability. We present zeta potential measurements of liposomes to measure the effective charge as well as membrane partitioning of SF by utilizing what we call an equi-activity analysis of several series of samples with different lipid concentrations. We observe an effective charge of −1.0 for SF at pH 8.5 and insignificantly lower at pH 7.4, illustrating that the effective charge may deviate strongly from the nominal value (−2 for 1 Asp, 1 Glu). The apparent partition coefficient decreases from roughly 100 to 20/mM with increasing membrane content of SF in agreement with the literature. Finally, by comparing zeta potentials measured soon after the addition of peptide to liposomes with those measured after a heat treatment to induce transmembrane equilibration of SF, we quantified the asymmetry of partitioning between the outer and inner leaflets. At very low concentration, SF binds exclusively to the outer leaflet. The onset of partial translocation to the inner leaflet occurs at about 5 mol-% SF in the membrane. This article is part of a Special Issue entitled: Interfacially Active Peptides and Proteins. Guest Editors: William C. Wimley and Kalina Hristova.

1. Introduction

We are interested in the mechanisms that ensure high fungicidal activity, sensitivity, and synergy of lipopeptides of the surfactin, fengycin, and iturin families produced by *Bacillus subtilis* QST713. This strain is successfully used for crop protection against a variety of fungal pathogens and there is strong evidence that the mode of action involves the permeabilization of the target cell membrane [1–5]. One of the key properties governing the behavior of these lipopeptides is their charge. Charged molecules are much more soluble and usually not spontaneously membrane-permeant. On the one hand, asymmetric insertion of an impermeant additive into the membrane causes "bilayer couple" effects that give rise to bending stress and, possibly, transient mechanical failure of the membrane [6–8]. On the other hand, the initiation of membrane pores may require a lipopeptide to reside in both membrane leaflets and may thus be kinetically hindered for impermeant peptides [1,9].

We describe a new strategy to conduct and evaluate zeta potential (ζ) measurements that accounts for partitioning effects and sheds light on the effective charge and membrane permeation of peptides and ionic surfactants. Measurements of electrophoretic mobility and electrostatic models have provided a wealth of insight into the binding of proteins, peptides, and small molecules to lipid membranes [10]. McLaughlin and co-workers showed early on [11] that zeta potentials of vesicles containing anionic lipids can be described by the Stern equation if one allows for a specific adsorption of certain ions to the charged surface. Comparing measurements of electrophoretic mobility (yielding ζ) with the binding of an anionic dye to the vesicle surface, these authors have also established that zeta potentials of vesicles can be used to derive surface potentials if one assumes the plane of shear to be 2 Å away from the surface [11].

These fundamental insights have permitted studying the electrostatic binding of peptides, drugs, ions, and other additives to membranes using zeta potential measurements [12]. Zeta potential measurements also revealed that calmodulin inhibitors can induce the release of electrostatically anchored proteins from the membrane by lowering the potential of cationic membrane patches [13]. The traditional approach to interpret zeta data in terms of membrane partitioning has been to measure ζ as a function of the additive concentration at fixed lipid content. The resulting curve is fitted by a Langmuir isotherm [14–16] or a Langmuir–Hill curve [17] or alternatively, transformed to ζ versus square root of concentration for a linear fit [18]. The apparent partition coefficient or binding constant of an additive is thus derived

☆ This article is part of a Special Issue entitled: Interfacially Active Peptides and Proteins. Guest Editors: William C. Wimley and Kalina Hristova.

* Corresponding author at: Leslie Dan Faculty of Pharmacy, University of Toronto, 144 College st, Toronto, ON M5S3M2, Canada.
E-mail address: heiko.heerklotz@utoronto.ca (H. Heerklotz).

http://dx.doi.org/10.1016/j.bbamem.2014.02.018
0005-2736/

based on its effective charge and additional, more or less physically meaningful parameters. Matos and coworkers compared such results with those of alternative partitioning experiments and found good agreement in most but not all cases [14,15,19]. Klasczyk et al. [20] obtained important, qualitative insight into metal ion binding to membranes but restrained themselves wisely from a quantitative evaluation, given the substantial experimental errors. This classical approach to interpret zeta data is limited by the problem that the effective charge number of a membrane-bound molecule may be affected by (de) protonation effects induced by intra- and intermolecular interactions and specific counterion and dipole effects that make it differ from the nominal value and render it hard to predict or measure. Such partial charge compensation has also been reported for SF before [21].

Since the surface potential affects the local concentration of an ionic surfactant or peptide at the membrane surface and, hence, the apparent partition coefficient from bulk, membrane binding data can provide information about the effective charges of membrane additives as well. A good example is the fit of isothermal titration calorimetry data on the basis of the Gouy–Chapman model [22–24]. Although this model makes a number of non-trivial assumptions, it was found to represent the binding isotherms astonishingly well. However, the effective charge corresponding to the best fit may deviate from the nominal charge. Insights into the charge state of membrane additives have also been obtained from NMR measurements detecting their effects on the orientation of neighboring lipid head groups (molecular voltmeter concept) [25].

We demonstrate that one can avoid any assumptions regarding the effective charge or partitioning model by what we refer to as an equiactivity analysis. It is based on quantifying how much more of an additive is needed to induce the same effect or membrane activity (e.g., induce a zeta potential of −20 mV) at higher lipid concentration. To our knowledge, this robust and largely model-independent approach has not been used so far to interpret zeta potential data. It is, however, very well established for fluorescence data from different dyes [26–28], leakage data [29,30], and phase transitions [31]; for a review see [32]. The only assumption it requires is that the observable is unequivocally related to the membrane composition represented, for example, by the additive-to-lipid mole ratio in the membrane, R_b. As a result of this procedure, one obtains the zeta potential as a function of R_b and, in turn, the effective charge numbers of additive and lipid. For additives with moderate apparent partition coefficients, the method provides also a model-free partitioning isotherm and, hence, composition-dependent apparent partition coefficient.

Another very interesting feature of zeta potential measurements is that they report, virtually exclusively, the concentration of peptide or surfactant in the outer leaflet of the liposomes. Comparing the local peptide or surfactant concentration in the outer leaflet after an addition with that after artificial transmembrane homogenization provides valuable insight into its membrane asymmetry and concentration-dependent membrane permeability.

2. Materials and methods

2.1. Materials

Large unilamellar vesicles were made from 1-palmitoyl-2-oleoyl-3-sn-glycero-phosphatidylcholine (POPC), which was a kind gift from Lipoid GmbH, Ludwigshafen (Germany). The surfactin fraction of the lipopeptides produced by *Bacillus subtilis* QST713 was kindly provided by Bayer CropScience, Davis CA.

All samples were made using Millipore water for preparing Tris buffer, 10 mM, including 100 mM NaCl and adjusted to pH 7.4 or 8.5. These materials were purchased from Sigma (Oakville, ON) or BioShop Canada Inc. (Burlington, ON) in the highest available purity.

Large unilamellar liposomes with a diameter of approximately 100 nm were produced by extrusion as described [1]. Briefly, an appropriate amount of lipid dissolved in chloroform was dried to a thin film by a gentle stream of nitrogen, followed by the exposure to vacuum overnight. Then, the appropriate amount of buffer was added, the lipid dispersed by vortexing, and the sample homogenized by 8 freeze-thaw cycles. Extrusion was done 15 times through Nuclepore polycarbonate filters of 100 nm pore size in a LIPEX Extruder (Northern Lipids, Burnaby BC) at room temperature.

The liposome size was monitored by dynamic light scattering using a Malvern Nano ZS. Previous phosphorus assays indicated that a gravimetric determination of the lipid has to take into account one water to remain bound per lipid (i.e., an effective molar mass of 778 g/mol POPC) and that the lipid concentration is essentially unchanged upon extrusion.

2.2. Zeta potential measurements

Measurements were made in a Malvern Nano ZS zeta sizer based on dynamic light scattering. The system works according to the PALS (phase analysis light scattering) principle, and the data are automatically evaluated on the basis of the Smoluchowski equation (the particle size of ≈100 nm is much larger than the Debye length, ≈1 nm). The sample was thermostated to 25°C by a built-in Peltier device. Measurements were made in standard disposable cuvettes using Malvern's dip cell.

Typically, a series of samples was prepared showing a constant lipid concentration and increasing concentrations of the lipopeptide. After adding appropriate amounts of a stock dispersion of lipid vesicles into a lipopeptide solution of the desired concentration, a sample was incubated for 1 h at 25°C. Then the zeta potential was measured to assess the state without additional equilibration procedures. Subsequently, transbilayer equilibration of the surfactant was realized by heat treatment, i.e., heating the sample under nitrogen to 65°C for 1 h, followed by cooling back to the experimental temperature, 25°C. There is good evidence that the enhanced temperature stimulates the flip-flop of membrane-bound surfactants across POPC bilayers, including ionic ones [23,33]. After the heat treatment, the zeta potential was measured again.

Each measurement was done in triplicate and the standard deviation of the results is shown as error bars in Fig. 1. It should be noted that the instrument may suffer from occasional outliers or systematic errors that build up and may cause biased yet reproducible and mutually consistent readings. Such effects may arise from deposits on the electrodes or contacts of the dip cell, air bubbles, or other problems (see also [17]). To ensure the validity of the data, a zeta standard was measured every 30 min. When the results showed poor reproducibility, unusual scatter compared to others in the same curve, or turned out to provide a poor resolution of $\zeta(c_S)$, additional samples were produced during the measurement to provide better statistics.

3. Theory

To model the experimental data, we need to derive a relationship between zeta potential and peptide content on the liposome surface. Charged head groups of the peptide (here, subscript SF for surfactin) and, in the general case, lipid on the surface of a liposome give rise to a surface charge density, σ [18]:

$$\sigma(X_b) = \frac{e_0 \cdot [X_b z_{SF} + (1-X_b) z_L]}{X_b A_{SF} + (1-X_b) A_L} = e_0 \frac{z_L + R_b z_{SF}}{A_L + R_b A_{SF}}. \quad (1)$$

Here, z_{SF} and z_L represent the signed charge numbers of peptide and lipid and R_b and X_b denote the mole ratio and mole fraction of the peptide within the membrane, respectively. Then, $1 - X_b$ gives the mole fraction of lipid (the mole fractions of lipid and peptide in a binary system add up to 1). Hence, the numerator of Eq. (1) represents the weighted average of the electrostatic charge per lipid molecule on the

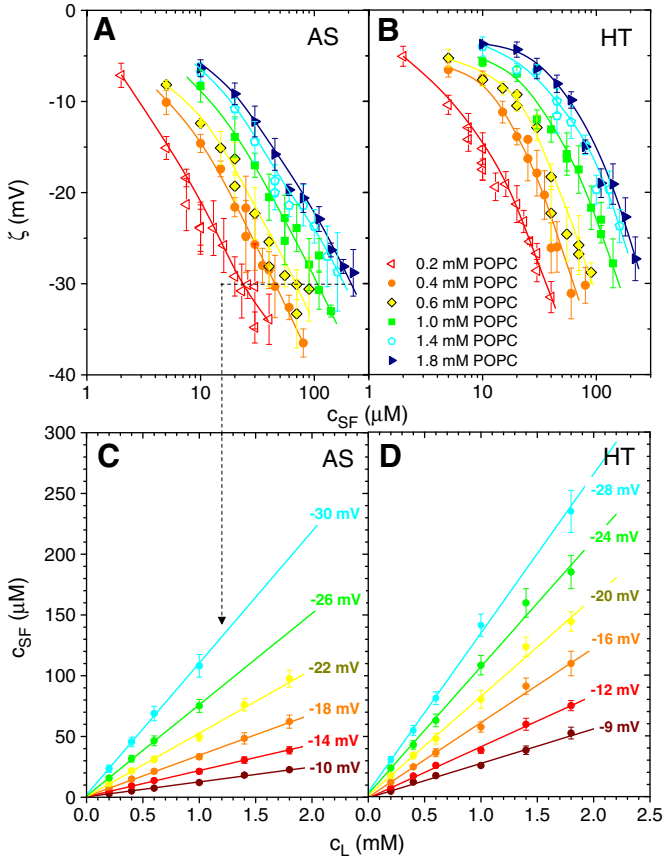

Fig. 1. Results of zeta potential measurements for series at certain lipid concentration (see legend in plot) as a function of the concentration of surfactin in the sample, c_{SF}, before (A) and after (B) heat treatment, respectively, as well as resulting equi-activity plots (C from A, D from B) with each data set showing pairs of c_{SF} and c_L that give rise to the same interpolated zeta potential. Error bars reflect standard errors of at least 3 measurements and lines in A and B are to guide the eye only. The intersection points of these arbitrary curves with the dotted grid line in A yield the ordinate values of the −30 mV — equi-activity data set in panel C. Equi-activity-data are fitted using Eq. (5) to yield the parameters collected in Fig. 3A.

surface. The denominator gives the average area per lipid molecule, considering the interfacial areas per peptide and lipid, A_{SF} and A_L, respectively.

One of the experimental observables that shed light on σ is the zeta potential, ζ. It depends on σ as well as on the partial screening of the related potential by the ions in the layer of aqueous solution that travels with the liposome. The screening depends on the reciprocal Debye length of the solution, κ, the effective thickness of the surface-immobilized layer, δ, and the permittivity of the medium, $\varepsilon_r\varepsilon_0$. For low absolute values of the zeta potential up to about ±25 mV, Gouy–Chapman theory implies the relationship:

$$\zeta = \sigma \frac{\exp\{-\kappa\delta\}}{\kappa\varepsilon_0\varepsilon_r}. \tag{2}$$

The Debye length, in turn, depends on the ionic strength, I, of the solution as:

$$\kappa^{-1} = \sqrt{\frac{\varepsilon_0\varepsilon_r kT}{2N_A e^2 I}} \tag{3}$$

with:

$$I = \frac{1}{2}\sum_i c_i z_i^2 \tag{4}$$

yielding a value of $1/\kappa = 9$ Å for an ionic strength of 105 mM and $\varepsilon_r = 80$. The index i sums over all charged components in solution, with the respective concentrations c_i and charge numbers z_i. The effective distance of the plane of shear of the surface-immobilized layer from the surface has been reported as $\delta = 2$ Å [10,18].

4. Results

4.1. Zeta potentials after asymmetric and equilibrated insertion of peptide

Fig. 1A shows the zeta potential of liposomes as a function of SF concentration for several series differing in lipid concentration. The samples were measured 1 h, respectively, after pipetting a small amount of a vesicle dispersion of 40 mM lipid into a peptide solution of the desired concentration to a total of 1 mL. Since the peptide is potentially membrane impermeant, its insertion into the membrane is possibly asymmetric as indicated by the symbol "AS".

As expected, the partitioning of SF into the membrane renders ζ increasingly negative. Since ζ is related to the surface charge density, a larger peptide concentration, c_{SF}, is needed to induce a given ζ at higher lipid concentration, c_L. The curves in Fig. 1A, B are arbitrary representations of the data, drawn considering the individual error bars of the data points.

Fig. 1B shows the zeta potential measured for the same samples as in Fig. 1A yet after a "heat treatment" (symbol HT) at 65°C for 1 h, followed by re-equilibration at 25°C. There is good evidence that this treatment stimulates a fast flip-flop of all membrane components, including those with bulky polar and ionic headgroups [23,33]. The fact that part of the bound peptide leaves the outer leaflet of the liposomes, where it contributes to ζ, for the inner leaflet is reflected by the observation that the curves in Fig. 1B are shifted to lower ζ or higher c_{SF} compared to those in Fig. 1A.

4.2. Equi-activity analysis to derive ζ as a function of membrane-bound peptide

The dotted line in Fig. 1A intersects with all curves at ζ = −30 mV. The abscissa values of the interpolated intersection points of the six curves with the dotted line are plotted as cyan points in Fig. 1C, as a function of the lipid concentration corresponding to each zeta curve. The linear relationship $c_{SF}(\zeta = -30\ \text{mV})$ versus c_L is a consequence of the mass balance for the lipopeptide (total concentration c_{SF}), which is either bound (concentration c_{SF}^b) or free in aqueous solution (concentration c_{SF}^{aq}):

$$c_{SF} = c_{SF}^b + c_{SF}^{aq} = R_b c_L + c_{SF}^{aq}. \tag{5}$$

The second equality includes the mole ratio of bound lipopeptide to lipid in the membrane, $R_b = c_{SF}^b/c_L$. Eq. (5) represents, indeed, a straight line of $c_{SF}(c_L)$ if R_b and c_{SF}^{aq} are constant. We have fulfilled this condition by choosing conditions $c_{SF}(c_L)$ that all share the same ζ, because ζ is unequivocally related to the surface charge density and, hence, to R_b. If R_b is constant, the equilibrium bulk aqueous concentration is given by the apparent partition coefficient, K_{app}:

$$K_{app} \equiv \frac{R_b}{c_{SF}^{aq}} \tag{6}$$

and, hence, constant as well. For the cyan points in Fig. 1C derived from the −30 mV-"equi-activity line", a linear fit yields a slope of $R_b = 0.11 \pm 0.01$ and $c_{SF}^{aq} = (2 \pm 4)$ μM. The errors given here are standard errors

of the fit that take into account the errors of the individual points as estimated from the uncertainty of reading a c_{SF} for a given ζ in panels A and B (error bars in panels C and D). The same procedure was applied at several other ζ values, yielding additional equi-activity lines (Fig. 1C) and, hence, values of R_b, c_{SF}^{aq}, and K_{app} for the selected ζ (collected in Figs. 3, 4).

What is crucial for our current study is that in contrast to substantial possible errors of c_{SF}^{aq} and K_{app}, the precision of the R_b values is generally excellent (see R_b-errors shown in Fig. 5A) and the data are therefore very suitable for deriving a partitioning-corrected zeta curve, ζ(R_b).

4.3. Kinetics of transmembrane equilibration

We have discussed the fact that the translocation of the charged lipopeptide from the directly accessible, outer leaflet of the vesicles to the inner membrane leaflet reduces the absolute value of ζ. Here we present a quick test whether this fact can be utilized for an estimate of the translocation rate.

Fig. 2 shows ζ measurements as a function of time after exposing the liposomes to 3 different lipopeptide concentrations (open symbols). After 100 h, the liposomes were heat treated to induce transbilayer equilibration and measured once more (solid symbols).

The so-obtained reference values for complete translocation were used as final values, $\zeta(t \rightarrow \infty)$, in a monoexponential fit. Only for the sample with 30 μM SF, we used the lower limit of the error range to improve the overall fit. At 15 μM SF, the corresponding overall fraction of lipopeptide in the membrane is 2.3 mol-% and, hence, a starting value of 4.6 mol-% in the outer leaflet. The translocation is very slow with a lifetime of the order of 45 h. At higher mole fractions of 4.3 mol-% (30 μM) and 11 mol-% (70 μM), translocation is significantly faster with lifetimes of 17 h and 8 h, respectively, but a truly quantitative evaluation is not possible because the differences between the points are not strictly significant in the first place. A large-scale series of experiments could reduce the experimental errors and hence improve the significance and precision of the fits but this is beyond the scope of the current paper.

5. Discussion

5.1. Effective charge of SF in the membrane

The previous section has derived zeta potential as a function of the mole fraction of SF in the membrane as plotted in Fig. 3A. As long as

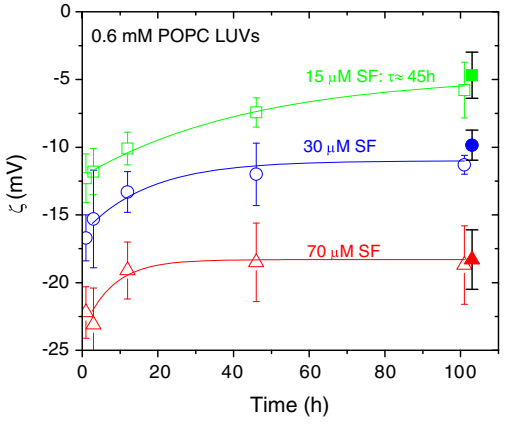

Fig. 2. Time dependence of the zeta potential after mixing for 15 μM (squares), 30 μM (circles), and 70 μM (triangles) SF in liposome suspensions of 0.6 mM. Solid symbols represent measurements after heat treatment and are assumed to reflect samples with the lipopeptide equilibrated between the outer and inner leaflets. Curves correspond to monoexponential fits (see text).

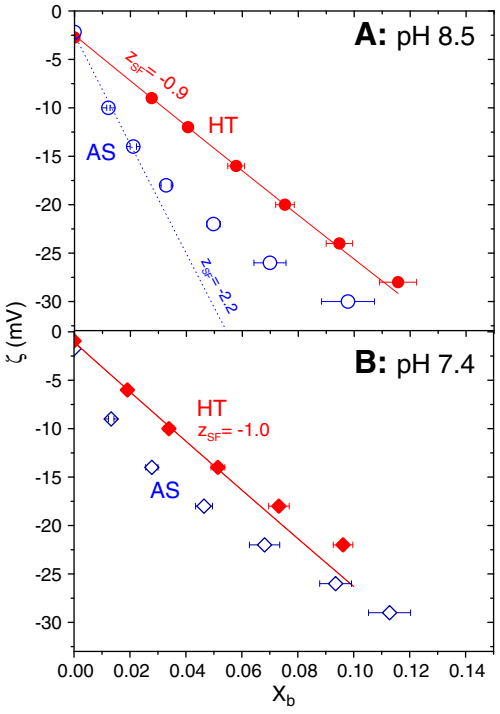

Fig. 3. Zeta potential (ζ) of vesicles as a function of the mole fraction of bound SF in the membrane, X_b. Solid symbols refer to experiments after heat treatment, open ones refer to the same samples before heat treatment that might show an asymmetric insertion of SF, favoring the outer lipid leaflet of the vesicles. The points in panel A were derived from the equi-activity analysis shown in Fig. 1C,D; panel B refers to analogous, independent measurements at pH 7.4 (raw data not shown).

the effective charge numbers of SF and lipid are constant, this line can be fitted by

$$\zeta\left(X_{SF}^{b}\right) = b(\kappa,\delta)e_0 \frac{X_b z_{SF} + (1-X_b)z_L}{X_b A_{SF} + (1-X_b)A_L} \tag{7}$$

as derived from Eq. (2) with (Eq. 1) and the constant factor of $b(\kappa,\delta)e_0 = 1.7 \times 10^4$ mV Å^2. The latter value corresponds to a monovalent electrolyte of 110 mM ($\kappa^{-1} = 9.3$ Å) using Eqs. (3) and (4). The distance between the plane of shear, where the electrostatic potential is ζ, and the surface was assumed to be $\delta = 2$ Å as published [10,18].

The solid red line illustrates a fit of Eq. (7) to the data for $|\zeta| < 25$ mV as obtained after heat treatment. It yields $z_{SF} = -0.9$ and $z_L = -0.01$ for pre-set values of A_L: = 65 Å^2 (from [34]) and A_{SF}: = 30 Å^2 ([21], see below). As expected [10], the limitations of the linearized model, Eq. (2), cause deviations from the fit at higher absolute values of ζ.

Discussing the precision and validity of the fit parameters, it should be noted that the low peptide content in the membrane renders the fit very little sensitive to A_{SF}. The value of 30 Å^2 used in the first fit represents a minimum found for tight packing of SF in pure SF monolayers [21]. The optimal partial area of SF in a membrane is most likely larger, including for example area contributions from neighboring lipids due to SF-induced disordering effects [33]. Such area changes were seen for other surfactants [35] but not quantified, to our knowledge, for SF yet. However, a fit using an arbitrarily chosen value of $A_{SF} = 80$ Å^2 still yields an effective charge of −0.9. The fit is also rather stable when the distance of the slipping plane from the membrane surface, δ, is concerned. Assuming a value of $\delta = 1$ Å implies $b(\kappa,\delta)e_0 = 1.9 \times 10^4$ mV Å^2 and yields a fitted charge number of $z_{SF} = -0.8$. For $\delta = 3$ Å, $b(\kappa,\delta)e_0 = 1.5 \times 10^4$ mV Å^2 and z_{SF} becomes −1.0 so that overall, we find $z_{SF} = -0.9 \pm 0.1$ for δ varying from 1 to 3 Å.

Fig. 3 contains a second data set (open symbols), which has been measured after a one hour incubation after adding SF stock solution to

POPC vesicles yet without a homogenization of the two membrane leaflets by a heat treatment. The initial slope is considerably larger because the outer leaflet contains virtually all bound SF, about twice the total bound amount. Instead of formally fitting this curve (which would yield $z_{SF} \approx -2.2$), we use these data to derive the accessibility parameter, γ, below.

Fig. 3B shows the analogous results obtained at pH 7.4. The fit parameters, $z_{SF} = -1.0$ and $z_L = -0.004$, are very similar to those at pH 8.5 and, again, virtually independent of A_{SF} and δ.

The results of these experiments imply that only one of the two acidic residues, Glu and Asp, of SF carries an effective charge, whereas the other one is protonated or compensated by a counterion over a broad pH range from at least 7.4 to 8.5. This is consistent with the results of Maget-Dana and Ptak [21] who estimated from Langmuir monolayer experiments that SF interacts with Na^+ to reach a degree of ionization of 0.3–0.4, i.e., $z_{SF} \approx -0.7$, at pH 9 and 150 mM NaCl. A slightly higher ionization as obtained in our study is to be expected if the anionic lipopeptides are interspersed between zwitterionic lipids rather than interacting strongly with each other (but note also lower salt in our case). A less-than-nominal charge of SF is also in line with an NMR structure [36] showing a saddle-like shape of the peptide cycle with the two acidic residues in close proximity — in spite of their potential electrostatic repulsion. It, finally, explains why ITC partitioning experiments for SF could be modelled with a rather constant apparent partition coefficient over a substantial concentration range, a finding that was at variance with the nominal charge of −2 if applied [37].

Summarizing this section, SF studied here is another example for the phenomenon that effective charges of peptides and other molecules may deviate strongly from the expected nominal charge on the basis of their ionizable groups and their individual pK_a values. This is a problem for predicting solubility, membrane selectivity, composition-dependence of partitioning, membrane permeability, and many other crucial properties of membrane-active compounds. It also challenges the validity of partitioning data derived from zeta potential measurements at a single lipid concentration. All these problems can be resolved by a direct determination (and consideration) of the effective charge using the equi-activity-approach demonstrated here.

5.2. Membrane permeability and asymmetry

So far, we have discussed the results of heat-treated samples that are assumed to represent liposomes with virtually equal concentrations of SF in the outer and inner lipid leaflets. However, zeta potential measurements provide also an interesting opportunity to study membrane asymmetry because they detect the charged compounds in the outer leaflet selectively.

The selective binding to the outer leaflet has been described using an "accessibility factor", γ, to rescale the overall lipid concentration to the accessible fraction of it [22,38]. For impermeant molecules added to LUV, $\gamma = 0.5$; to small vesicles it may rather be 0.6 since the outer leaflet is significantly larger than the inner and contains about 60% of the lipid. We redefine the parameter such that:

$$\gamma \equiv \frac{R_b}{R_b^{out}} \tag{8}$$

where R_b represents the overall mole ratio of bound peptide per lipid at a given point in time. Note that this is kinetically controlled upon partial translocation to the inner leaflet(s) and not necessarily an equilibrium quantity. R_b^{out} denotes the local mole ratio in the outer leaflet or, generally, in the fraction of lipid that is equilibrated with the aqueous solution. In the extreme cases of perfect asymmetry and full equilibration discussed above, this definition yields the same values for γ as the classic one of 0.5 for impermeable and 1 for permeable LUV, respectively. Definition (8) generalizes the concept to include partial equilibration. If, for example, the local mole ratio is 0.6 in the outer but, after partial equilibration, 0.2 in the inner leaflet of an LUV, γ as defined here is $0.5 \cdot (0.6 + 0.2) / 0.6 = 0.67$.

In order to estimate γ in the experiments without heat treatment, we may consider a pair of R_b values, obtained with and without heat treatment, respectively, at any common ζ: $R_b(HT, \zeta)$ and $R_b(AS, \zeta)$. Since ζ is the same and ζ is a function of the local composition of the outer leaflet, we may conclude that

$$R_b^{out}(HT, \zeta) = R_b^{out}(AS, \zeta) \tag{9}$$

and with Eq. (8) we may substitute $R_b^{out}(AS,\zeta)$ for $R_b(AS,\zeta)/\gamma$. The analogous substitution applies also to $R_b^{out}(HT,\zeta)$, but here we assume that the heat treatment has equilibrated the sample and $\gamma = 1$. Solving the substituted eq. for γ, we obtain:

$$\gamma = \frac{R_b(AS, \zeta)}{R_b(HT, \zeta)}. \tag{10}$$

For example, for SF at pH 7.4, we find in Fig. 3 that an arbitrarily chosen $\zeta = -14$ mV has been obtained for X_b (AS) = 0.028 and X_b(HT) = 0.051. While mole fractions were the more convenient abscissa for Fig. 3, we have to convert these values into mole ratios now with the general conversion $R_b = X_b / (1 - X_b)$, yielding R_b(AS, −14 mV) = 0.029 and R_b(HT, −14 mV) = 0.054. With Eq. (10), γ = 54% which means that the membranes are highly asymmetric and only about half of the lipid is accessible to surfactin. Fig. 4 shows the γ values obtained for different ζ values, both for pH 7.4 and 8.5. Both curves start at $\gamma \approx 0.4$ at low lipopeptide concentration, which can be interpreted in terms of a small fraction of bi- or oligolamellar vesicles and no flip-flop of SF to the inner leaflet(s). At $X_b \approx 0.05$, γ starts to increase suggesting an increasing extent of translocation to the inner leaflet within the incubation time of the experiment. This partial translocation of SF has previously been concluded from ITC data [37] and coincides with the onset of membrane leakage for aqueous solutes [4]. The induced flip that causes the concentration dependent increase in γ is slightly weaker at pH 8.5 compared to pH 7.4. This is expected for a slightly larger charge number at pH 8.5 which is in line with Fig. 3, but the difference is not significant given experimental errors.

5.3. Membrane partitioning

Partitioning isotherms, such as $R_b(c_{SF}^{aq})$, and apparent partition coefficients, K_{app}, can directly be obtained from the fits in Fig. 1C,D for sufficiently large R_b and not too large K_{app}, where the error of the y-intercept, c_{SF}^{aq}, is acceptable. Fig. 5A shows that up to at least R_b of 0.06, c_{SF}^{aq} values are indistinguishable from zero and yield no more than a lower limit of K_{app}, for example $K_{app} > 50$ mM^{-1} for $R_b = 0.05$ and $c_{SF}^{aq} = 0 \pm 1$ μM. At higher concentrations, one can get explicit estimates

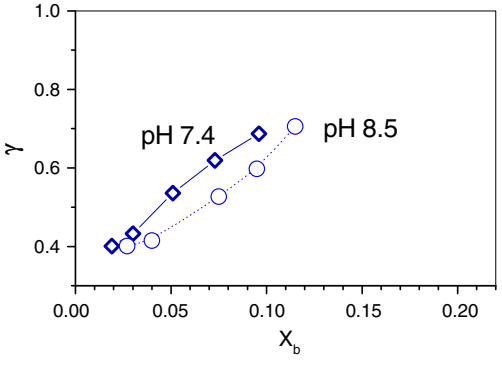

Fig. 4. The asymmetry of SF partitioning into the outer and inner membrane leaflets about 1 h after addition of SF as represented by the accessibility parameter, γ, as a function of the average mole fraction of SF in the membrane, X_b. Spheres refer to pH 8.5, diamonds to pH 7.4. Accessibility γ is obtained from the data in Fig. 3 using Eq. (10).

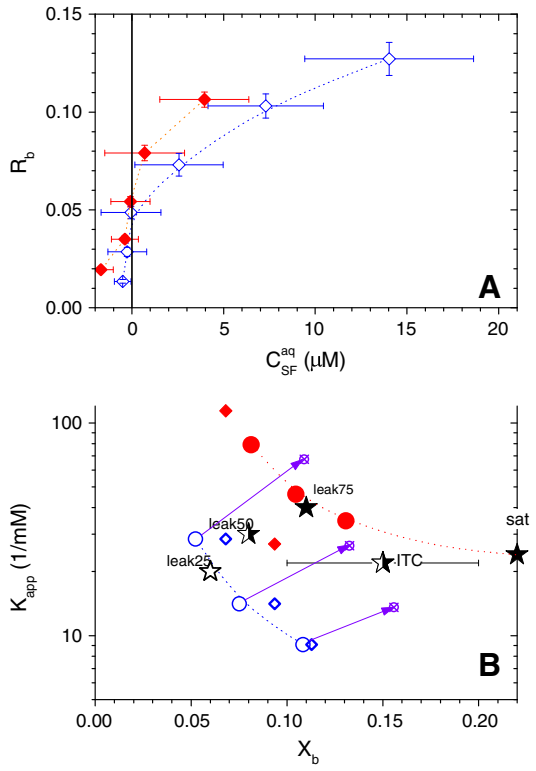

Fig. 5. Binding isotherms for surfactin to POPC membranes at pH 8.5 (A) and membrane composition dependent, apparent partition coefficients (B) as obtained from equi-activity fits including those shown in Fig. 1C,D. Solid symbols refer to samples after heat treatment, open ones refer to findings without heat treatment. Spheres refer to pH 8.5, diamonds to pH 7.4. Error bars illustrate standard errors of the linear equi-activity fits. Stars represent literature values obtained with little (open), partial (half-open) and substantial (solid) transmembrane equilibration of surfactin by leakage measurements ("leak", numbers give degree of de-quenching of entrapped dye, [4]), ITC uptake experiments ("ITC", [37]), and lipid-dependent membrane saturation ("sat", [4]). The arrows illustrate the corrections $K_{app} \rightarrow K_{app}/\gamma$ and $R_b \rightarrow R_b/\gamma$ (abscissa converted to mole fraction X_b) using γ values from Fig. 4 that should shift the open symbols (asymmetric measurement) approximately to the range of the equilibrium data (solid symbols); see text.

for K_{app} as shown in Fig. 5B. Comparison with literature data and internal consistency imply that, at least for SF as studied here, these estimates are better than expected on the basis of standard errors of c_{SF}^{aq} and R_b.

Let us first discuss the results obtained after heat treatment (Fig. 1D), which are assumed to reflect close to equilibrium distribution of the peptide within the membrane and yield the solid symbols in Fig. 5B. K_{app} decreases from ≈100/mM at ≈7 mol-% to ≈30–50/mM at ≈10–13 mol-%, the differences between the data at pH 8.5 (spheres) and 7.4 (diamonds) are probably within experimental error. The decrease of K_{app} is a consequence of the increasingly negative surface potential that opposes further incorporation of the anionic SF. The results are in surprisingly good agreement with literature values for SF from another strain of *Bacillus* at pH 8.5 as illustrated by solid stars. Agreement is also found with the values obtained from steady-state leakage experiments for 75% de-quenching (i.e., largely but perhaps not fully equilibrated samples) and from ITC solubilization experiments at saturation (label "sat").

Naturally, uncorrected K_{app} values obtained for asymmetric insertion (K_{app}(AS)) of an impermeant molecule without heat treatment, major leakage, or other mechanism of transbilayer equilibration are smaller than those obtained after heat treatment (K_{app}(HT)), because only a fraction γ of the lipid is truly accessible for partitioning. This is indeed seen for the open symbols in Fig. 5B as derived from Fig. 1C, which are found in agreement with literature data for weak leakage. Literature data for partial equilibration (half-solid stars) obtained by ITC partitioning experiments and for 50% de-quenching range between open and solid symbols, as one should expect.

Typically, one corrects partitioning data obtained upon outside addition of an impermeant solute by calculating K_{app}(AS)/γ to estimate the equilibrium value. At a closer look, there are a number of problems that may limit the precision of such an estimate. First, for a concentration-dependent K_{app}, the effective X_b has to be corrected as well (correction $R_b \rightarrow R_b/\gamma$). Second, assuming $\gamma = 0.5$ for LUV is not perfect given the possibility of a few oligolamellar vesicles and of partial flip-flop as illustrated in Fig. 4. Taking these points into account, we have corrected the open spheres (data for pH 8.5 without heat treatment) in Fig. 5B as illustrated by the arrows. The so-corrected values agree with the points obtained after heat treatment within error, particularly at lower X_b. At this point, it should be mentioned that there is a third issue with the correction that could not be taken into account quantitatively here. As discussed, asymmetric membrane insertion of amphiphiles creates what is referred to as "bilayer couple" stress; additive insertion is opposed (decreasing K_{app}) if it increases this stress and promoted if it relaxes it [6].

Overall, we may stress that our approach yielded a decrease in K_{app}(HT) from ≈80/mM at 8 mol-% to ≈30/mM at 13 mol-%, in good agreement with literature values.

6. Conclusions

1) Zeta potential measurements of peptides and other additives binding to liposomes can be corrected for partitioning effects using an equi-activity analysis as used for other observables before.
2) The equi-activity analysis permits the determination of the effective charge of a membrane additive, as opposed to knowing or guessing it as an input value to traditional fit procedures. For surfactin, we obtained the apparent charge number of -1.0 ± 0.1 which deviates strongly from the nominal charge of −2, illustrating that guessing effective charges can be quite misleading.
3) Since zeta potential represents the additive in the outer membrane leaflet, it indicates non-equilibrium partitioning and the permeation threshold for an additive. Asymmetry-driven permeation of surfactin across the membrane starts at about 5 mol-%.
4) The equi-activity analysis yields an estimate for the apparent partition coefficient of surfactin of, e.g., 30/mM at 13 mol-%; this is in very good agreement with literature data.

Acknowledgement

We thank Bayer CropScience in Davis, CA, particularly Jon Margolis, David Sesin, Dorte Lindhard and Jorge Jimenez, for providing lipopeptide samples as well as invaluable scientific and technical advice and support. We are indebted to Stuart McLaughlin, Sandro Keller, and Sylvio May for very helpful comments. We acknowledge the zeta potential measurements performed by Roshan Tahavori and Badria Anis in the frame of undergraduate research projects. This work was made possible by the financial support from the Natural Sciences and Engineering Research Council of Canada (NSERC) and from Bayer CropScience (Davis, CA).

References

[1] H. Patel, C. Tscheka, K. Edwards, G. Karlsson, H. Heerklotz, All-or-none membrane permeabilization by fengycin-type lipopeptides from *Bacillus subtilis* QST713, Biochim. Biophys. Acta 1808 (2011) 2000–2008.
[2] M. Ongena, P. Jacques, Bacillus lipopeptides: versatile weapons for plant disease biocontrol, Trends Microbiol. 16 (2008) 115–125.
[3] M. Deleu, M. Paquot, T. Nylander, Effect of fengycin, a lipopeptide produced by *Bacillus subtilis*, on model biomembranes, Biophys. J. 94 (2008) 2667–2679.
[4] H. Heerklotz, J. Seelig, Leakage and lysis of lipid membranes induced by the lipopeptide surfactin, Eur. Biophys. J. 36 (2007) 305–314.

[5] A. Grau, J.C. Gomez Fernandez, F. Peypoux, A. Ortiz, A study on the interactions of surfactin with phospholipid vesicles, Biochim. Biophys. Acta 1418 (1999) 307–319.
[6] H. Heerklotz, Membrane stress and permeabilization induced by asymmetric incorporation of compounds, Biophys. J. 81 (2001) 184–195.
[7] M.P. Sheetz, S.J. Singer, Biological membranes as bilayer couples. A molecular mechanism of drug–erythrocyte interactions, Proc. Natl. Acad. Sci. U. S. A. 71 (1974) 4457–4461.
[8] S. Esteban-Martin, H. Jelger Risselada, J. Salgado, S.J. Marrink, Stability of asymmetric lipid bilayers assessed by molecular dynamics simulations, J. Am. Chem. Soc. 131 (2009) 15194–15202.
[9] S.M. Gregory, A. Cavenaugh, V. Journigan, A. Pokorny, P.F.F. Almeida, A quantitative model for the all-or-none permeabilization of phospholipid vesicles by the antimicrobial peptide cecropin A, Biophys. J. 94 (2008) 1667–1680.
[10] S. McLaughlin, The electrostatic properties of membranes, Annu. Rev. Biophys. Biophys. Chem. 18 (1989) 113–136.
[11] M. Eisenberg, T. Gresalfi, T. Riccio, S. McLaughlin, Adsorption of monovalent cations to bilayer membranes containing negative phospholipids, Biochemistry 18 (1979) 5213–5223.
[12] J. Kim, M. Mosior, L.A. Chung, H. Wu, S. McLaughlin, Binding of peptides with basic residues to membranes containing acidic phospholipids, Biophys. J. 60 (1991) 135–148.
[13] P. Sengupta, M.J. Ruano, F. Tebar, U. Golebiewska, I. Zaitseva, C. Enrich, S. McLaughlin, A. Villalobo, Membrane-permeable calmodulin inhibitors (e.g. W-7/W-13) bind to membranes, changing the electrostatic surface potential: dual effect of W-13 on epidermal growth factor receptor activation, J. Biol. Chem. 282 (2007) 8474–8486.
[14] H. Ferreira, M. Lucio, J.L. Lima, C. Matos, S. Reis, Effects of diclofenac on EPC liposome membrane properties, Anal. Bioanal. Chem. 382 (2005) 1256–1264.
[15] C. Matos, B. de Castro, P. Gameiro, J.L. Lima, S. Reis, Zeta-potential measurements as a tool to quantify the effect of charged drugs on the surface potential of egg phosphatidylcholine liposomes, Langmuir 20 (2004) 369–377.
[16] C. Matos, C. Moutinho, P. Lobao, Liposomes as a model for the biological membrane: studies on daunorubicin bilayer interaction, J. Membr. Biol. 245 (2012) 69–75.
[17] N. Kaszas, T. Bozo, M. Budai, P. Grof, Ciprofloxacin encapsulation into giant unilamellar vesicles: membrane binding and release, J. Pharm. Sci. 102 (2013) 694–705.
[18] T. Schaffran, J. Li, G. Karlsson, K. Edwards, M. Winterhalter, D. Gabel, Interaction of N, N, N-trialkylammonioundecahydro-closo-dodecaborates with dipalmitoyl phosphatidylcholine liposomes, Chem Phys Lipids 163 (2010) 64–73.
[19] C.M. Matos, J.L.C. Lima, S. Reis, A. Lopes, M. Bastos, Interaction of antiinflammatory drugs with EPC liposomes: calorimetric study in a broad concentration range, Biophys. J. 86 (2004) 946–954.
[20] B. Klasczyk, V. Knecht, R. Lipowsky, R. Dimova, Interactions of alkali metal chlorides with phosphatidylcholine vesicles, Langmuir 26 (2010) 18951–18958.
[21] R. Maget-Dana, M. Ptak, Interfacial properties of surfactin, J. Colloid Interface Sci. 153 (1992) 285–291.
[22] J. Seelig, P. Ganz, Nonclassical hydrophobic effect in membrane binding equilibria, Biochemistry 30 (1991) 9354–9359.
[23] S. Keller, H. Heerklotz, A. Blume, Monitoring lipid membrane translocation of sodium dodecyl sulfate by isothermal titration calorimetry, J. Am. Chem. Soc. 128 (2006) 1279–1286.
[24] S. Keller, H. Heerklotz, N. Jahnke, A. Blume, Thermodynamics of lipid membrane solubilization by sodium dodecyl sulfate, Biophys. J. 90 (2006) 4509–4521.
[25] P.M. Macdonald, J. Seelig, Anion binding to neutral and positively charged lipid membranes, Biochemistry 27 (1988) 6769–6775.
[26] M. Encinas, E. Lissi, Evaluation of partition constants in compartmentalized systems from fluorescence quenching data, Chem. Phys. Lett. 91 (1982) 55–57.
[27] H. Heerklotz, H. Binder, G. Lantzsch, G. Klose, Membrane/water partition of oligo(ethylene oxide) dodecyl ethers and its relevance for solubilization, Biochim. Biophys. Acta 1196 (1994) 114–122.
[28] M. Paternostre, O. Meyer, C. Grabielle-Madelmont, S. Lesieur, M. Ghanam, M. Ollivon, Partition coefficient of a surfactant between aggregates and solution: application to the micelle–vesicle transition of egg phosphatidylcholine and octyl beta-D-glucopyranoside, Biophys. J. 69 (1995) 2476–2488.
[29] A. De La Maza, J.L. Parra, M.T. Garcia, I. Ribosa, J.S. Leai, Permeability changes in the phospholipid bilayer caused by nonionic surfactants, J. Colloid Interface Sci. 148 (1992) 310–316.
[30] H. Patel, C. Tscheka, H. Heerklotz, Characterizing vesicle leakage by fluorescence lifetime measurements, Soft Matter 5 (2009) 2849–2851.
[31] D. Lichtenberg, Characterization of the solubilization of lipid bilayers by surfactants, Biochim. Biophys. Acta 821 (1985) 470–478.
[32] H. Heerklotz, Interactions of surfactants with lipid membranes, Q. Rev. Biophys. 41 (2008) 205–264.
[33] M. Nazari, M. Kurdi, H. Heerklotz, Classifying surfactants with respect to their effect on lipid membrane order, Biophys. J. 102 (2012) 498–506.
[34] J.F. Nagle, S. Tristram-Nagle, Structure of lipid bilayers, Biochim. Biophys. Acta 1469 (2000) 159–195.
[35] G. Lantzsch, H. Binder, H. Heerklotz, Surface area per molecule in lipid/C12En membranes as seen by fluorescence resonance energy transfer, J. Fluoresc. 4 (1994) 339–343.
[36] J.M. Bonmatin, M. Genest, M.C. Petit, E. Gincel, J.P. Simorre, B. Cornet, X. Gallet, A. Caille, H. Labbe, F. Vovelle, et al., Progress in multidimensional NMR investigations of peptide and protein 3-D structures in solution. From structure to functional aspects, Biochimie 74 (1992) 825–836.
[37] H. Heerklotz, J. Seelig, Detergent-like action of the antibiotic peptide surfactin on lipid membranes, Biophys. J. 81 (2001) 1547–1554.
[38] H. Heerklotz, J. Seelig, Titration calorimetry of surfactant-membrane partitioning and membrane solubilization, Biochim. Biophys. Acta 1508 (2000) 69–85.